Original Research Article

Synthesis and FTIR analysis of Cd Doped Nano Ni - Aluminates

ABSTRACT

Nano Ni – Aluminates ($Ni_{0.5}$ $Fe_{0.5}$ Al_2O_4) and Cd Doped Nano Ni – Aluminates ($Ni_{0.5}$ $Fe_{0.5}$ Al_{2-x} Cd_xO_4) where x = 0.2, 0.4, 0.6 and 0.8 were synthesized by co-precipitation method. Ammonium hydroxide was used as precipitating agent. The samples were characterized using Fourier transform infrared spectroscopy. FTIR spectrum for each unannealed sample of $Ni_{0.5}$ $Fe_{0.5}$ Al_2 O_4 and $Ni_{0.5}$ $Fe_{0.5}$ Al_{2-x} Cd_x O_4 exhibit a broad band near 3450 cm^{-1} due to –OH stretching vibration of free hydrogen bonded hydroxyl group and a second typical absorption band at 1620 cm^{-1} resulting from deformative vibration of water molecules. Spectra for samples after annealing show peaks in the range of 900-450 cm^{-1} and 850-500 cm^{-1} showing presence of Al-O and Ni-O bonds respectively thus confirm the formation of metal oxides bonds while no peak was observed for –OH bond. A peak around 420 cm^{-1} is assigned to Cd-O bond.

Keywords:Nano-Ni Aluminates, Cd doped Nano Ni-aluminates, Co-precipitation, Fourier Transform Infrared Spectroscopy

1. INTRODUCTION

Nanotechnology is a broad concept which provides wide range of exceptional cases to alter the world. This technology deals with particles having dimensions at a length scale of 1 / 100 million of a meter [1]. This specific field allows molecular diagnosis at nanoscale. Nanotechnology integrates chemistry, biology and material sciences to create novel properties that can be exploited to attain new market opportunities and challenges. Industrial perspectives cover electronics, biomedical, performance materials and consumer products. Nanotechnology offers applications in cancer therapy [2], dental materials [3], optics, DNA engineering, high performance textiles, catalysis and sports.

Materials having internal or space surface structure in the nanoscale are represented as nanomaterials. Nanomaterials complexity provides a diversity of functions to products [4]. Nanoparticles are fundamental components of nanomaterials. Nanomaterials are divided into various categories depending on dimension, size, morphological parameters, structure and basic composition. Metal based nanoparticles are synthesized from metals to nanometric sizes using constructive or destructive methods [5]. Metal NPs include silver(Ag), gold(Au), Iron(Fe), aluminum(Al), cadmium(Cd), cobalt(Co), copper(Cu), lead(Pb). Reduction of size of particles to nanometer scale alters the band gap, creating discrete energy levels with the large number of active atoms due to greater separation among the atomic-coordinates and un-saturated points. These metal based nanomaterials have biomedical applications [6] such as catheters implants, medical delivery system, tissue engineering and dentistry.

Various metal oxides (Fe_2O_3, Al_2O_3, TiO_2, ZnO and SiO_2) can be prepared using sol-gel or hydrothermal method [7]. Variation in different morphological characteristics alter band gap energies of the materials. Modification of surface can be done using a polymeric precursor chain, coupling reagents or doped with metallic ionic species, epoxies, amines, thiols and anionic compounds. Metal oxide nanoparticles have attractive applications in the field of catalysis, sensors, electronics, environmental remediation, biotechnology, magnetic fluids, data storage devices, and magnetic resonance imaging [8].

Semiconductor nanomaterials are made up of different compounds of various groups including IV A group (SiO_2) [9]. These nanomaterials have 4ev bandgap energy [9]. Unique quantum nature of these nanomaterials [10] enhances their physical and chemical properties. They have many applications including transparent conductive contact, varistor, solar cell, luminescent devices, laser diodes and UV-lasers. Nanomaterials can be classified according to their dimensionality [11]. This classification mode depends upon size of nanoparticles which range from one to 100nm in one dimension. 0D nanomaterials have size below 100 nm [12], with all their dimensions in nanoscale. Spherical, cube, nano-rod, polygon, hollow sphere, metal and core shell nanomaterials are included in this group. Quantum dots are well known member of this group. QDs are semiconductor [13], metal oxides having 1000 to 100,000 atoms in an extended solid structure. They have enhanced electronic, optical, magnetic and catalytic properties. 1D nanomaterials [14] have at least single dimension which is not in nanoscale but remaining two dimensions in nanometric range. One dimensional nanomaterials [15] include metallic, polymeric, ceramic, nanotubes and nano-rod filaments. Nanowires and nanofibers are well known examples of this group. Nanowires have single crystal structure with a diameter of a few tens of nanometers [16]. These are widely used in electronic devices as nano-interconnector for transport of electrons.

2D nanomaterials [17] have at least single dimension of nanometric range but remaining two dimensions are not in nano scale. These involve single layered, multilayered crystals, amorphous thin layered surfaces, nano plates and nanocoatings. Layered silicates are novel field within nanotechnology for nanoscale engineering of surfaces and layers with exceptional functionalities and physical effects. 3D nanomaterials [18] include many dimensions above 100 nanometer. Examples include foam, fiber, CNTs, fullerene, polycrystals, layered skeletons, honeycombs structures, pillars.

Nano Crystalline Spinels [19] are Face centered cubic close packing of anionic particles possessing holes provide the special structure of nano crystalline spinel. These holes are partially filled by cations particles. They have molecular formula (A^{2+}) $[B_2{}^{3+}]O_4{}^{2-}$ While A^{2+} and B^{3+} are the divalent and trivalent cations at tetrahedral (A) and octahedral (B) interstitial sites of the face centered cubic aroused by O^{2-} ions [20]. Different parameters of these oxides depend upon the type and positions of these cations among the two interstitial sites. Ionic bond is present in all oxide spinel. Calcining temperature is the controlling factor for different types of spinels. Based on distribution of cations among two interstitial sites, nanocrystalline spinels are divided into following types of Normal spinel, Inverse spinel, Random spinel [21]. The main aspect of normal spinel is the presence of A^{2+} in tetrahedral position and B^{3+} in octahedral position [22]. Example includes $CoAl_2O_4$. This double oxide spinel finds its applications in ceramics, glasses, paints and T.V tubes. In Inverse Spinel, half of trivalent ion preferentially fill the tetrahedral sites (A site) and other half occupies the octahedral sites (B site). Example includes $NiAl_2O_4$ and can be represent as: $(Al^{3+})_A\,[Ni^{2+}Al^{3+}]_B\,O_4{}^{2-}$ where A is tetrahedral site and B is octahedral site [23]. Nickel aluminates attract the research interest because of excellent thermal stability [24], high mechanical resistance, hydrophobicity and lower surface acidity. In random spinel, tetrahedral and octahedral interstitial sites are randomly occupied by the two metallic ions (A^{2+}, B^{3+}). Example includes $MgFe_2O_4$.

Nanomaterials are of special interest because of their novel applications in different field of sciences [25]. Surface modification with various type of functional groups and active agents create definite active site thus enhancing surface topography. Surface interactions including noncovalent, covalent, electrostatic wander walls or hydrogen bonding made nanomaterials functionalized for different applications and fields. Nanoparticles serve as a bridge between bulk material and atomic or molecular structures. Novel properties of nanoparticles are governed by their significantly smaller size. Size controls fundamental electric, magnetic, mechanical and thermal properties without changing their chemical composition. There are several methods for synthesis of nanoparticles. Co-precipitation method involves nucleation, growth, coarsening and agglomeration to take place at the same time of chemical reaction [26]. Insoluble precipitates of product are formed owing to high supersaturation. Coarsening and agglomeration affect size, shape and properties of particles. This is an important route for synthesis of metals, oxides and metal chalconides with easy and rapid precipitation without any organic reagent at a relatively low temperature. Nanoparticles with desired shape, size and morphology can be obtained. This method is useful to synthesize super ionic materials, microporous crystals, chemical sensor products, electronics, ceramics, magnetic and luminescence items. This is a green chemistry approach for fabrication of porous metal oxide spheres [27]. Sufficient templating is obtained for providing monodispersed, nonagglomerated porous spheres. Fe and Al_2O_3 sols result in cracked spheres having sufficient oxide material on surface while in case of Indium oxide, a hollow broken shell is obtained which are more active photocatalyst than Degussa P_{25} titania (a commercial standard). Mesoporous silica films can serve as template for gold and platinum nanoparticles having uniform size distribution [28]. Biological synthesis interconnects nanotechnology and biotechnology to synthesize large variety of NPs. Diversity of biological materials bring the method important from economical point of view. Synthesis of Au, Ag, Au-Ag alloys, Se, Te, Pt, Pd, Si, Ti, Zr, QDs nanoparticles using bacteria, algae, fungi, yeast and viruses is commonly employed nowadays. This method is not commercially important owing to slow rate of synthesis

having poly dispersed nanoparticles. Photobiological method provides sufficient yield with improved properties [29].

2. EXPERIMENTAL DETAILS

2.1. Solution

First of all, 0.1M stock solution of nickel nitrate, 0.1M stock solution of Iron (III) nitrate, 0.2M stock solution of aluminum nitrate and 5M stock solution of ammonium hydroxide were prepared for synthesis of undoped and cadmium doped nano aluminates. Ammonium hydroxide stock solution serves as a precipitating agent for precipitate formation.

Calculation for stock solutions is listed below:

Table 1. Stock solutions

Chemical formula of compound	Molarity	Mass of metal salt (g) in 100mL
$Ni(NO_3)_2.6H_2O$	0.1	2.90
$Fe(NO_3)_3.9H_2O$	0.1	4.04
$Al(NO_3)_3.9H_2O$	0.2	7.50

2.2. Preparation of undoped and Cd-doped Nano Ni-aluminates

To prepare undoped and cadmium doped nano aluminates, concentration of nickel nitrate and iron (III)nitrate were kept same while that of aluminum nitrate was different as follows:

$$Ni_{0.5}\ Fe_{0.5}\ Al_{2-x}\ Cd_x\ O_4$$

There are following formulas for cadmium doped nano aluminates:

- $Ni_{0.5}\ Fe_{0.5}\ Al_{1.8}\ Cd_{0.2}\ O_4$
- $Ni_{0.5}\ Fe_{0.5}\ Al_{1.6}\ Cd_{0.4}\ O_4$
- $Ni_{0.5}\ Fe_{0.5}\ Al_{1.4}\ Cd_{0.6}\ O_4$
- $Ni_{0.5}\ Fe_{0.5}\ Al_{1.2}\ Cd_{0.8}\ O_4$

2.2.1 Stoichiometric calculations

2.2.1.1 Calculation for $Ni_{0.5}\ Fe_{0.5}\ Al_{1.8}\ Cd_{0.2}\ O_4$

Calculation for aluminum nitrate solution

Solution of aluminum nitrate for x=0.2 Composition, having molarity 0.09M was prepared from 0.2 M stock solution of aluminum nitrate. 112.5ml solution was taken from 0.2 M stock solution of aluminum nitrate in a 250mL measuring flask and filled with distilled water to prepare 0.09M solution.

Calculation for cadmium nitrate

A : B :: C : D
0.1 : 2 :: y : 0.2

(2) (y) = (0.1) (0.2)

y = (0.1) (0.2)/2

y = 0.01M

A = 0.1M of Al $(NO_3)_3$ used , B = Stoichiometric amount of $Al(NO_3)_3$
C = Molarity of Cd $(NO_3)_2$ to be required, D = Stoichiometrically required ratio of $Cd(NO_3)_2$
1000mL water consist amount of $Cd(NO_3)_2$= 308.50g
1mL water consist amount of $Cd(NO_3)_2$ =(308.50/1000)

250mL water consist amount of $Cd(NO_3)_2$ = (308.50/1000) x (250)= 77.125g

0.01M consist amount of $Cd(NO_3)_2$ = (77.125) x (0.01) = 0.77125g

2.2.1.2 Calculation for $Ni_{0.5}\ Fe_{0.5}\ Al_{1.6}\ Cd_{0.4}\ O_4$

Calculation for aluminum nitrate solution

Solution of aluminum nitrate for x=0.4 composition having molarity 0.08M was prepared using 100mL solution from 0.2M stock solution of aluminum nitrate and poured in a 250mL measuring flask and then filled with distilled water up to the mark.
Calculation for cadmium nitrate

A : B :: C : D
0.1 : 2 :: y : 0.4
(2) (y) :: (0.1) (0.4)
(y) :: (0.1) (0.4)/2
y = 0.02M

A = 0.1M of Al $(NO_3)_3$ used, B = Stoichiometric amount of $Al(NO_3)_3$
C = Molarity of Cd $(No_3)_2$ to be required, D = Stoichiometrically required ratio of $Cd(NO_3)_2$
1000mL water consist amount of $Cd(NO_3)_2$= 308.50g
1mL water consist amount of $Cd(NO_3)_2$ =308.50/1000
250mL water consist amount of $Cd(NO_3)_2$ = (308.50/1000) x (250) =77.125
0.02M water consist amount of $Cd(NO_3)_2$ = (77.125) x (0.02) =1.5425g

2.2.1.3 Calculation for $Ni_{0.5}\,Fe_{0.5}\,Al_{1.4}\,Cd_{0.6}\,O_4$
Calculation for aluminum nitrate solution
Solution of aluminum nitrate for x=0.6 composition with molarity 0.07 was prepared using 87.5mL solution from 0.2M stock solution of aluminium nitrate in a 250mL measuring flask.
Calculation for $Cd(NO_3)_2$

A : B :: C : D
0.1 : 2 :: y : 0.6
(2) (y) = (0.1) (0.6)
y = (0.1) (0.6)/2
y = 0.03M

A = 0.1M of Al $(NO_3)_3$ used, B = Stoichiometric amount of $Al(NO_3)$
C = Molarity of Cd $(NO_3)_2$ to be required, D = Stoichiometrically required ratio of $Cd(NO_3)_2$
1000mL water consist amount of $Cd(NO_3)_2$= 308.50 g
1mL water consist amount of $Cd(NO_3)_2$ =308.50/1000
250mL water consist amount of $Cd(NO_3)_2$ = 308.50/1000x250 =77.125g
0.03M consists amount of $Cd(NO_3)_2$ = (77.125) x (0.03) = 2.31375g

2.2.1.4 Calculation for $Ni_{0.5}\,Fe_{0.5}\,Al_{1.2}\,Cd_{0.8}\,O_4$
Calculation for aluminum nitrate solution
Solution of aluminium nitrate for X=0.8, with molarity 0.06 was prepared using 75mL from 0.2M stock solution of aluminium nitrate in a 250mL measuring flask.

Calculation for $Cd(NO_3)_2$

A : B :: C : D

0.1 : 2 :: y : 0.8
(2) (y) :: (0.1) (0.8)
y = (0.1) (0.8)/2

y = 0.04M

A = 0.1M of Al $(NO_3)_3$ used
B = Stoichiometric amount of $Al(NO_3)_3$
C = Molarity of Cd $(NO_3)_2$ to be required
D = Stoichiometrically required ratio of $Cd(NO_3)_2$
1000mL water consist amount of $Cd(NO_3)_2$= 308.50 g
1mL water Consist amount of $Cd(NO_3)_2$ =(308.50/1000)
250mL water consist amount of $Cd(NO_3)_2$ = (308.50/1000) x (250) = 77.125g
0.04M water consist amount of $Cd(NO_3)_2$ = (77.125) x (0.04) = 3.085g
The above calculated amount of $Cd(NO_3)_2$ was added with nickel nitrate, iron nitrate & aluminum nitrate mixture. Stirring was done continuously to from a homogenous mixture before adding the precipitating agent. $Cd(NO_3)_2$ was added in five compositions gradually increases as x = 0.0, 0.2, 0.4, 0.6, 0.8

2.2.2 Solution Mixing
0.025M Solution of nickel nitrate (in measuring flask of 250mL) and 0.025M solution of iron (III) nitrate (in measuring flask of 250mL) and 0.2M solution of aluminum nitrate (in measuring flask of 250mL) were mixed in a 1000mL beaker. Solution was continuously stirred for about 5 minutes to get homogeneity. pH of the

resultant solution came out to be 3 (checked by a pH meter). For synthesis of cadmium doped nickel-iron-nano-aluminates, 0.025M solution of nickel nitrate, 0.025M solution of iron (III) nitrate, 0.2 M solution of aluminum nitrate and cadmium nitrate solution of composition x = 0.02, 0.4, 0.6, 0.8 in sequence were poured in every 1000mL beakers. When cadmium nitrate was mixed in the solution, solution turns to be Brownish.

2.2.3 Co-precipitation

After mixing of solution and stirring for about 5 minutes, precipitation was carried out by drop wise addition of ammonium hydroxide as a precipitating agent. Ammonium hydroxide was added with continuous stirring for 3 hours until the pH became 11. Finally, precipitates were obtained in the form of hydroxide after stirring of 3 hours. Reaction of ammonium hydroxide with aluminum nitrate and iron nitrate resulted formation of respective hydroxides at room temperature.

$$3NH_4OH + Al(NO_3)_2 \longrightarrow Al(OH)_3 + 3NH_4NO_3$$
$$2NH_4OH + Ni(NO_3)_2 \longrightarrow Ni(OH)_2 + 2NH_4NO_3$$
$$3NH_4OH + Fe(NO_3)_3 \longrightarrow Fe(OH)_3 + 3NH_4NO_3$$

2.2.4 Washing

After stirring, the solutions were kept for about 12 hours until all precipitates were settled. Solution above the precipitates was wasted and precipitates were washed with distilled water many times to get 7 pH. Filtration was not carried out to avoid contamination as well as loss of precipitates after washing was completed.

2.2.5 Drying

Precipitates were allowed to settle down after pH=7. They were separated by removing above liquid solution and kept in petri-dish. Precipitates were dried at room temperature and finally kept in oven for 24 hours at 70˚C for complete drying.

2.2.6 Grinding

Grinding of dry precipitates was done using a pestle mortar after washing it with detergents to make it free from impurities. Pestle mortar was dried before use. All the samples were weighed on weighing balance after grinding and kept in air tight, labelled sample bottle to avoid contamination.

2.2.7 Annealing

Annealing of sample was carried out by using ceramic crucible. Crucibles were washed and dried properly. After weighing along with their lids, crucibles were labelled at bottom using lead pencil. Sample with amount 1.00g, 1.90g, 1.79g, 1.90g, 1.65g with composition x=0, 0.2, 0.4, 0.6, 0.8 respectively were added in each crucible and placed in a furnace at 700 ˚C temperature for 6 hours.

After annealing hydroxides were transformed to oxides of various compositions. In the last, samples were characterized byFTIR.

$$4Al(OH)_3 \longrightarrow 2Al_2O_3 + 6H_2O$$
$$4Fe(OH)_3 \longrightarrow 2Fe_2O_3 + 6H_2O$$
$$Ni(OH)_2 \longrightarrow NiO + H_2O$$

3. RESULTS AND DISCUSSION

3.1 SEM Analysis of Nano Ni - Aluminates

An examining electron magnifying lens (SEM) is an electron magnifying instrument that checks the outer layer of an example with a focused light emission to get pictures of the material [30]. At the point when electrons contact particles in an example, they produce an assortment of signs that give data about the example's surface geography and piece. A picture is made by joining the place of the electron shaft with the power of the identified sign in a raster filter design [30].

The morphology of ($Ni_{0.5}$ $Fe_{0.5}$ Al_2O_4) revealed a consistent pattern in all cases, characterized by visible aggregation of tiny particles. This aggregation was detected at two different magnification levels: 2m and 20m. This behavior is most likely due to nearby particle contact and bonding, which is assisted by hydrogen bonding with water molecules [31]. Capillary action then comes into play during the drying process of the precursors, further improving particle cohesiveness.

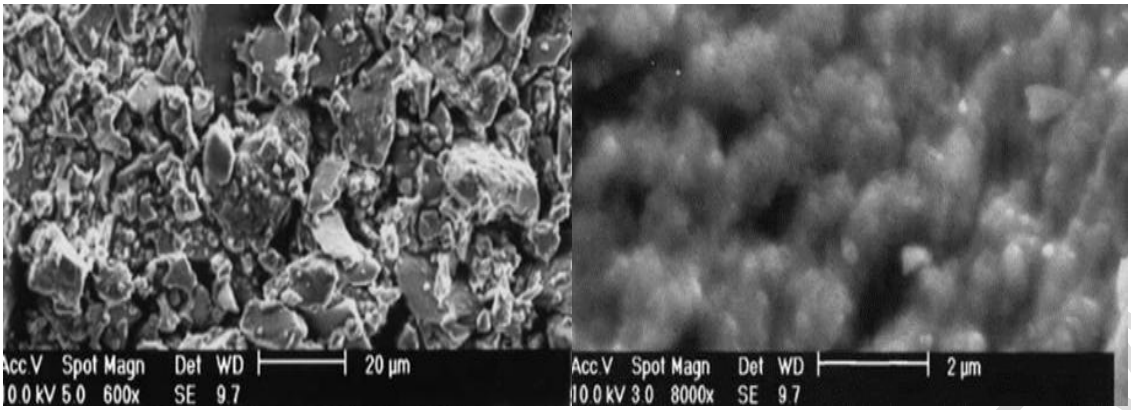

Fig. 1 SEM morphology of Nano Ni-Aluminates

3.2 UV-Visible Characterization of Cd doped Ni-aluminates

The UV-Visible spectra of Cd-doped nano Ni-Aluminates ($Ni_{0.5}$ $Fe_{0.5}$ Al_{2-x} Cd_xO_4) with varied x values (0.2, 0.4, 0.6, and 0.8) show the presence of four distinct absorption bands spanning diverse wavelength ranges: 230-370 nm, 350-400 nm, 586-669 nm, and 900-1250 nm. According to existing literature, the absorption peaks at 344 nm and 560 nm relate to charge exchanges between metal and oxygen atoms [32]. The absorption band from 586 to 669 nm is related with Ni^{2+} ions in a tetrahedral coordination, whereas the band from 900 to 1250 nm is associated with Ni^{2+} ions in an octahedral coordination [33].

Significant modifications are reported in Cd-doped $NiAl_2O_4$. Additional absorption bands appear between 430 and 580 nm, with a modest absorption range between 720 and 780 nm and a larger band stretching from 900 to 1250 nm. These modifications are linked to oxygen and cadmium charge transfer processes in both octahedral and tetrahedral locations. The last two wavelengths are associated with d-d transitions of Cd atoms in octahedral and tetrahedral positions, respectively. The complicated spectra represent nickel and Cd coexistence in these many coordination locations.

Light energy absorption at specific frequencies adds to the color of the material, changing the band gap [34]. The excitation of electrons from anionic to cationic bands causes the band gap to change. When Cd ions are introduced into $NiAl_2O_4$, a new electronic level is inserted between the valence band of O^{2-} and the conduction band of M^{2+}, resulting in a considerable reduction in band gap energy. This decrease is visible, with the energy decreasing from 3.11 eV to 2.63 eV. This effect is most likely caused by the electrical structure of the Cd^{2+} dopant, which induces a defect level within the band gap of the host lattice.

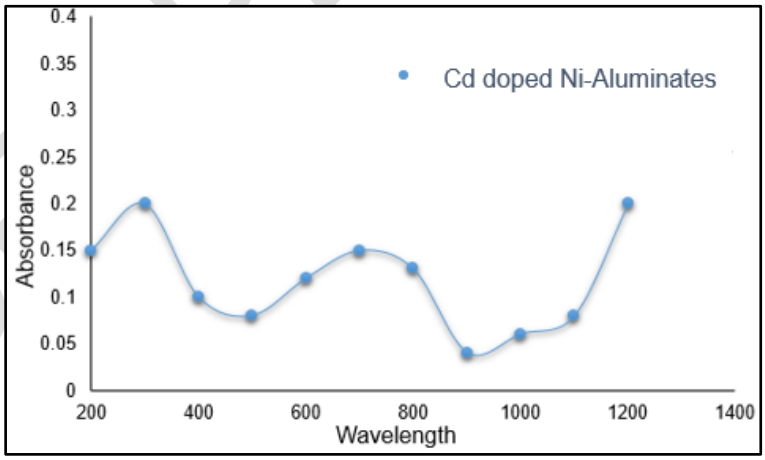

Fig. 2 UV-Vis Spectra of Cd doped Nano Ni-Aluminates

3.3 FTIR Analysis

Nano Ni-aluminates ($Ni_{0.5}Fe_{0.5}Al_2O_4$) and cadmium doped nano Ni-aluminates ($Ni_{0.5}Fe_{0.5}Al_{2-x}Cd_xO_4$) with (x = 0.2, 0.4, 0.6 and 0.8) were synthesized using coprecipitation method. Concentration of aluminum and iron show inverse trend toward concentration of cadmium nitrate. Stoichiometric amount of nickel nitrate, Iron nitrate and aluminum nitrate were used for synthesis of doped and undoped nano Ni-aluminates.

All prepared solutions with desired concentrations were well mixed in 1000 mL beaker and stirring was done continuously. A hot plate stirrer was also employed for about 5-10 minutes. Stoichiometric amount of cadmium nitrate, serving as doping agent, was added in solution of desired concentrations to synthesize

cadmium doped nano Ni-aluminates. In order to synthesize undoped nano Ni-aluminates, nickel nitrate, Iron nitrate and aluminum nitrate were mixed in ratio 1: 1: 2 respectively. Nickel nitrate and iron nitrate were in ratio 1:1 [35].

In case of cadmium doped nano aluminates, concentration of nickel and Iron were also kept constant but aluminum concentration was changed with reverse trend toward cadmium concentration. Stirring was done continuously to get a homogeneous solution. Ammonium hydroxide solution serving as precipitating agent [36], was poured dropwise continuously until pH was maintained at 11-12 as this pH was estimated to be ideal for hydroxide precipitate formation. The number and structure of complex, greatly depend on chemistry of metal ion being used and material properties change with change in pH [37] while 11-12 pH was estimated to be ideal for hydroxide precipitate formation [38] because nuclei coagulate together at this isoelectric point. By increasing pH, the powder float on the surface instead of settling down.

Solution was supported on magnetic hot plate stirrer during whole precipitation aided with continuous string at room temperature. After 6 hours, hydroxides were formed in the form of precipitates owing to ability of metal cations to form coordination compounds with hydroxide anion thus providing respective hydroxides.

$$3NH_4OH + Al(NO_3)_3 \longrightarrow Al(OH)_3 + 3NH_4NO_3$$
$$2NH_4OH + Ni(NO_3)_2 \longrightarrow Ni(OH)_2 + 2NH_4NO_3$$
$$3NH_4OH + Fe(NO_3)_3 \longrightarrow Fe(OH)_3 + 3NH_4NO_3$$

After removing from magnetic hot plate stirrer, solutions were kept for 12 hours until all precipitates were settled. Solution above precipitates was discarded and precipitates were separated and washed with deionized water until the pH was dropped to 7 to avoid any acidic or basis impurity. Precipitates were kept in Petri-dish and first dried in open air and finally placed in oven overnight at 70 °C temperature. Drying is preferentially done to allow heat to circulate uniformly for sufficient drying of precipitates.

A pestle mortar was employed for grinding dried precipitates into fine powder. Finally, this fine powder was analyzed by weight using weighing balance. After grinding fine powder, sample was kept in crucible and put in furnace at 700 °C for 6 hours. Water loss resulted in weight loss of sample powder, was observed when sample is weighed again after annealing. Hydroxides were converted into oxide with specific composition because of sufficiently high temperature treatment. Conversion of hydroxide into oxides disclosed some bond breaking, bond shifting and formation of some new bonds. As the rates of dissolution and precipitation are very slow at room temperature so annealing was done at sufficiently high temperature above boiling point to specific extent. Following oxides are expected to be formed during annealing at 700 °C for six hours.

$$2Al(OH)_3 \longrightarrow Al_2O_3 + 3H_20$$
$$2Fe(OH)_3 \longrightarrow Fe_2O_3 + 3H_2O$$
$$Ni(OH)_2 \longrightarrow NiO + H_2O$$

Table 2. Annealing of Samples

Sr no.	Compound composition (x)	Weight before annealing (g)	Weight after annealing (g)	Difference in weight (g)
1	0	1.00	0.84	0.16
2	0.2	1.90	1.53	0.37
3	0.4	1.79	1.60	0.19
4	0.6	1.90	1.68	0.22
5	0.8	1.65	1.24	0.41

Weight loss was observed owing to water removal during annealing as given in above table.

These oxides were subjected to grinding again to obtain find aluminates nanoparticles. A slight color change was observed as hydroxides (rust color) were converted to respective oxides. Oxides of nickel and Iron react with aluminum oxide to produce aluminates [39].

The obtained fine powder was filled in labeled air tight sample bottles and kept safe for FTIR.

FTIR analysis provides information about bonding and molecular structure. FTIR spectrum ranges from 400-4000 cm^{-1} and used to analyze and identify nature of prepared nanocrystalline spinel [40]. This technique was used to characterized nano Ni-aluminates and Cd doped nano Ni-aluminates. Both annealed and

unannealed samples were used to carry out FTIR analysis. FTIR spectra of $Ni_{0.5}\,Fe_{0.5}\,Al_2\,O_4$ and $Ni_{0.5}\,Fe_{0.5}\,Al_{2-x}\,Cd_x\,O_4$ with different compositions (x = 0.2, 0.4, 0.6, 0.8) before and after annealing are shown in figures 3 (a – j). FTIR spectrum for each unannealed sample of $Ni_{0.5}\,Fe_{0.5}\,Al_2\,O_4$ and $Ni_{0.5}\,Fe_{0.5}\,Al_{2-x}\,Cd_x\,O_4$ exhibit a broad band near 3450 cm^{-1} due to –OH stretching vibration of free hydrogen bonded hydroxyl group and a second typical absorption band at 1620 cm^{-1} resulting from deformative vibration of water molecules [41].

Spectra for samples after annealing show peaks in the range of 900-450 cm^{-1} and 850-500 cm^{-1} showing presence of Al-O and Ni-O bonds respectively thus confirm the formation of metal oxides bonds [42] and no peak was observed for –OH bond. A peak around 420 cm^{-1} is assigned to Cd-O bond [43].

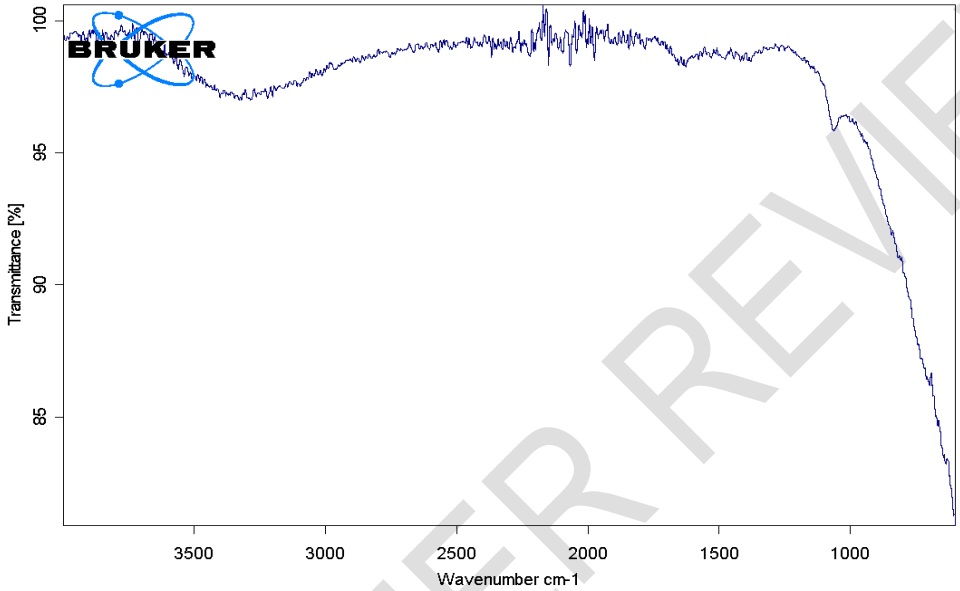

Figure 3. (a) FTIR Image of undoped $Ni_{0.5}\,Fe_{0.5}\,Al_2\,O_4$ (unannealed)

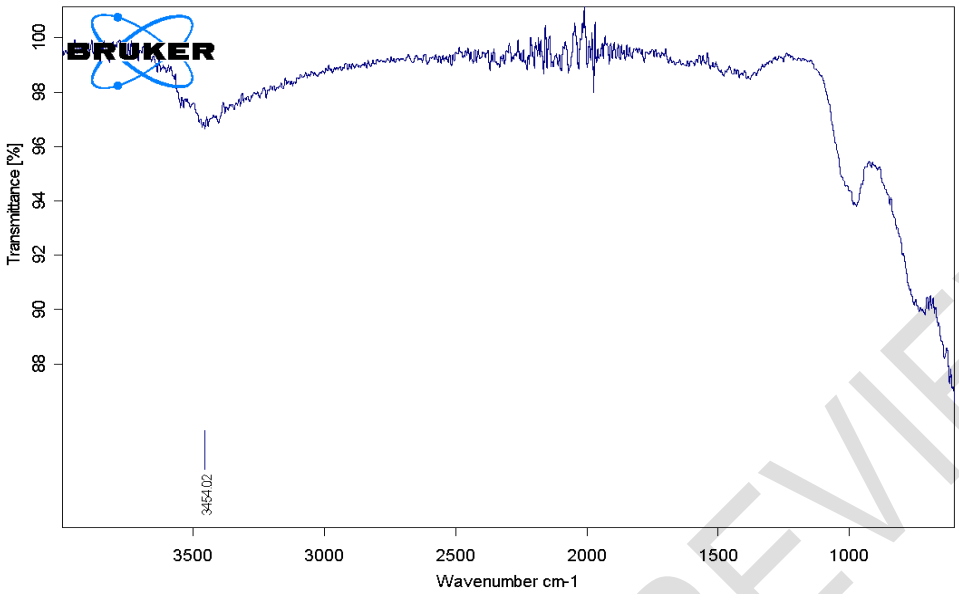

Figure 3. (b) FTIR Image of doped $Ni_{0.5}Fe_{0.5}Al_{1.8}Cd_{0.2}O_4$ (unannealed)

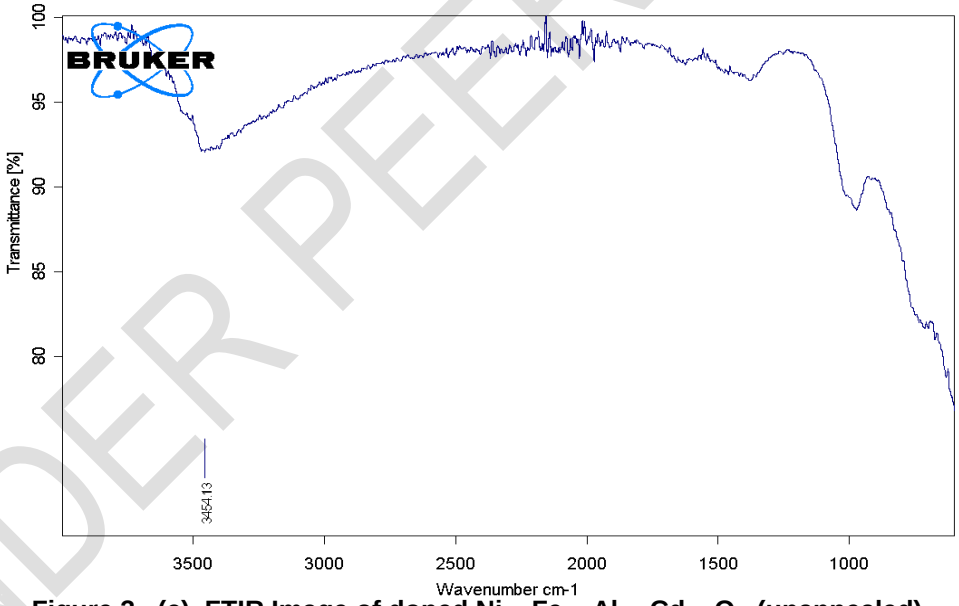

Figure 3. (c) FTIR Image of doped $Ni_{0.5}Fe_{0.5}Al_{1.6}Cd_{0.4}O_4$ (unannealed)

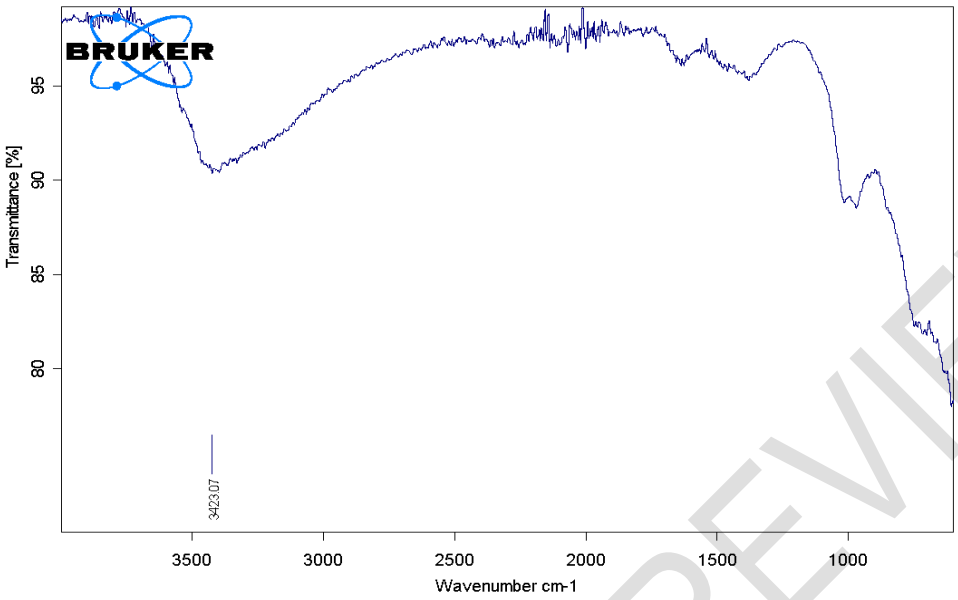

Figure 3 (d) FTIR Image of doped $Ni_{0.5}Fe_{0.5}Al_{1.4}Cd_{0.6}O_4$ (unannealed)

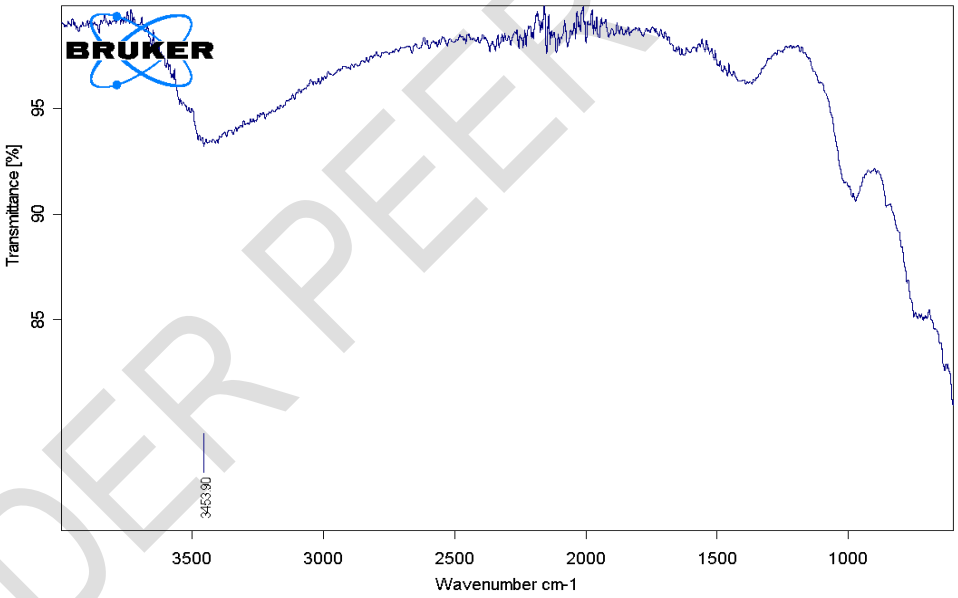

Figure 3 (e) FTIR Image of undoped $Ni_{0.5}Fe_{0.5}Al_{1.2}Cd_{0.8}O_4$ (unannealed)

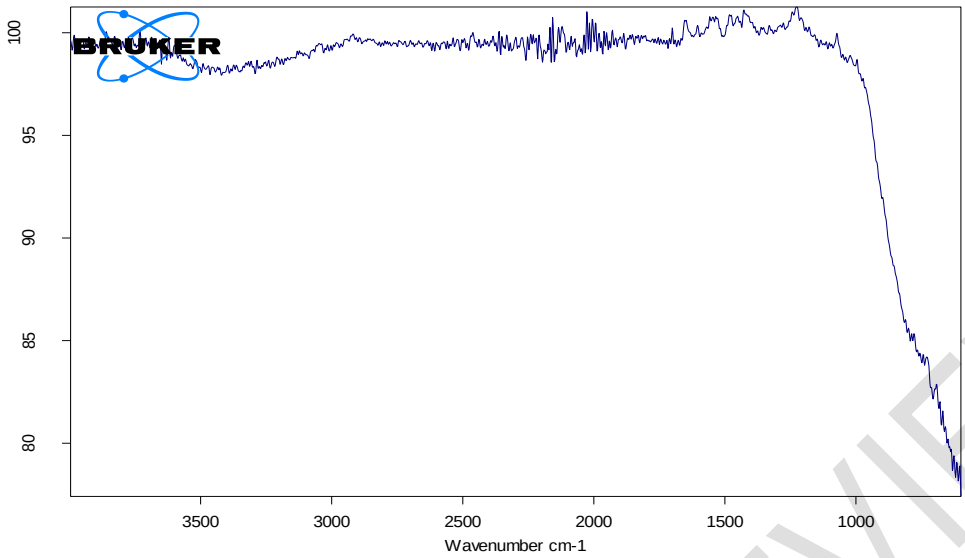

Figure 3 (f) FTIR Image of undoped $Ni_{0.5}Fe_{0.5}Al_2O_4$ (annealed)

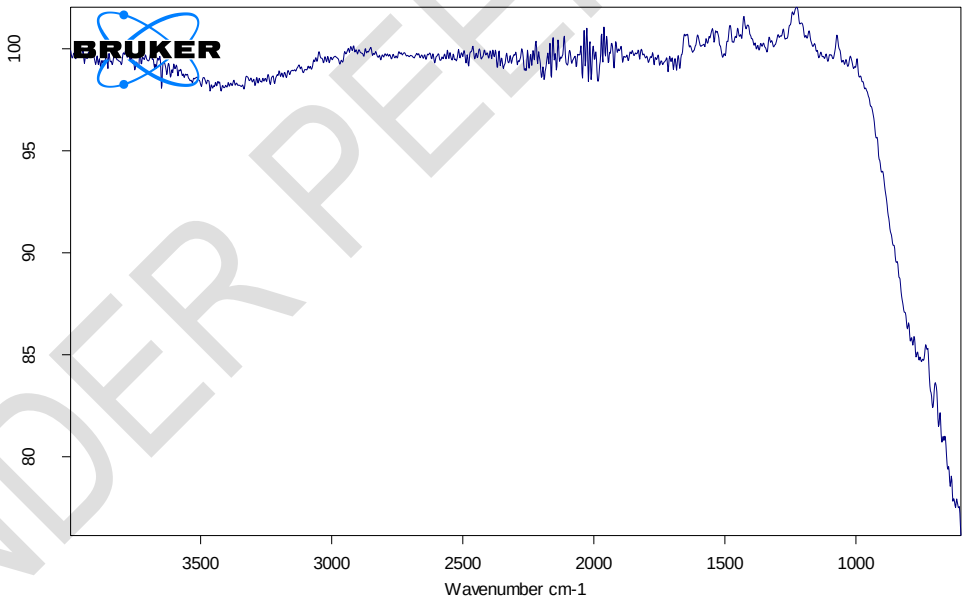

Figure 3 (g) FTIR Image of doped $Ni_{0.5}Fe_{0.5}Al_{1.8}Cd_{0.2}O_4$ (annealed)

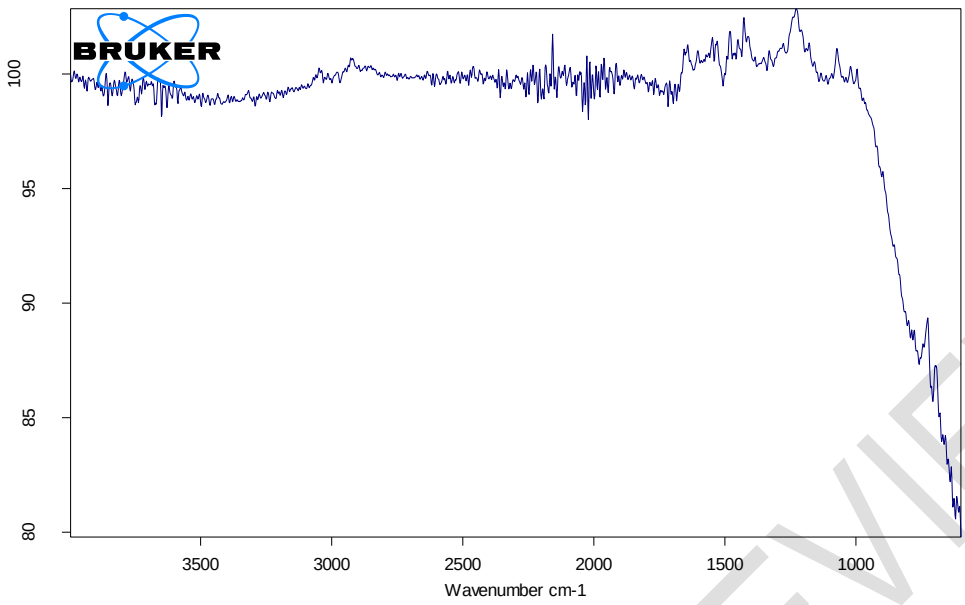

Figure 3 (h) FTIR Image of doped $Ni_{0.5}Fe_{0.5}Al_{1.6}Cd_{0.4}O_4$ (annealed)

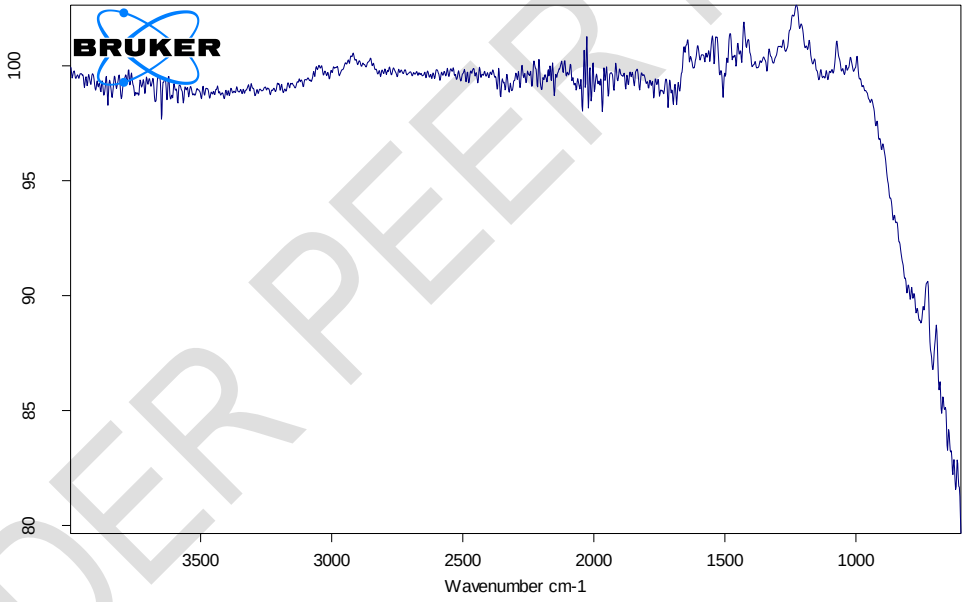

Figure 3 (i) FTIR Image of doped $Ni_{0.5}Fe_{0.5}Al_{1.4}Cd_{0.6}O_4$ (annealed)

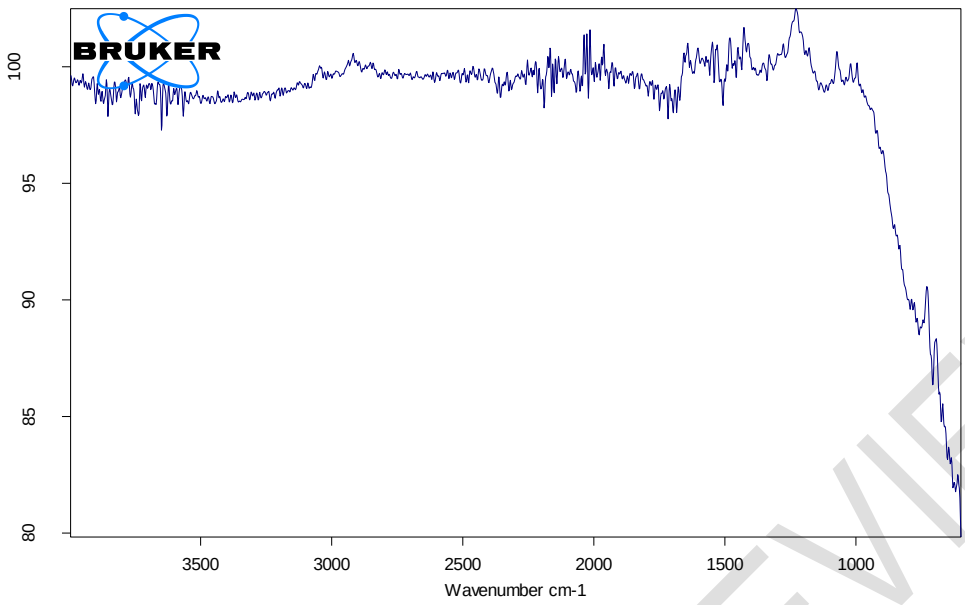

Figure 3 (j) FTIR Image of doped $Ni_{0.5}Fe_{0.5}Al_{1.2}Cd_{0.8}O_4$ (annealed)

4. CONCLUSION

Coprecipitation method was used to synthesize nano Ni-aluminates and cadmium doped nano Ni-aluminates. Ammonium hydroxide solution was used as precipitating agent. FTIR spectrum for each unannealed sample of $Ni_{0.5}$ $Fe_{0.5}$ Al_{2-x} Cd_x O_4 exhibit a broad band near 3450 cm^{-1} due to –OH stretching vibration of free hydrogen bonded hydroxyl group and a second typical absorption band at 1620 cm^{-1} resulting from deformative vibration of water molecules.

Spectra for samples after annealing show peaks in the range of 900-450 cm^{-1} and 850-500 cm^{-1} showing presence of Al-O and Ni-O bonds respectively thus confirm the formation of metal oxides bonds while no peak was observed for –OH bond. A peak around 420 cm^{-1} is assigned to Cd-O bond.

6. Declarations

Ethical Approval: Not applicable (NA)

Availability of data and materials: Not applicable (NA)

Ethics approval/declarations: Not applicable (NA)

Consent to participate. NA

Consent for publication. NA

Availability of data and material/ Data availability. NA

Code availability (software application or custom code). NA

REFERENCES

1. Wang, G., *Nanotechnology: The new features.* arXiv preprint arXiv:1812.04939, 2018.
2. Nie, S., et al., *Nanotechnology applications in cancer.* Annu. Rev. Biomed. Eng., 2007. **9**: p. 257-288.
3. McCabe, J.F. and A.W. Walls, *Applied dental materials*. 2013: John Wiley & Sons.

4. Champion, J.A., Y.K. Katare, and S. Mitragotri, *Making polymeric micro-and nanoparticles of complex shapes.* Proceedings of the National Academy of Sciences, 2007. **104**(29): p. 11901-11904.
5. Ijaz, I., et al., *Detail review on chemical, physical and green synthesis, classification, characterizations and applications of nanoparticles.* Green Chemistry Letters and Reviews, 2020. **13**(3): p. 223-245.
6. Makvandi, P., et al., *Metal-based nanomaterials in biomedical applications: antimicrobial activity and cytotoxicity aspects.* Advanced Functional Materials, 2020. **30**(22): p. 1910021.
7. Arora, A.K., et al., *Applications of metal/mixed metal oxides as photocatalyst:(A review).* Oriental Journal of Chemistry, 2016. **32**(4): p. 2035.
8. Chavali, M.S. and M.P. Nikolova, *Metal oxide nanoparticles and their applications in nanotechnology.* SN applied sciences, 2019. **1**(6): p. 607.
9. Sakthisabarimoorthi, A., S.M.B. Dhas, and M. Jose, *Fabrication and nonlinear optical investigations of SiO2@ Ag core-shell nanoparticles.* Materials Science in Semiconductor Processing, 2017. **71**: p. 69-75.
10. Muhammad, S., et al., *Quantum chemical design of nonlinear optical materials by sp 2-hybridized carbon nanomaterials: issues and opportunities.* Journal of Materials Chemistry C, 2013. **1**(35): p. 5439-5449.
11. Sannino, D., *Types and classification of nanomaterials.* Nanotechnology: Trends and Future Applications, 2021: p. 15-38.
12. Asha, A.B. and R. Narain, *Nanomaterials properties*, in *Polymer science and nanotechnology*. 2020, Elsevier. p. 343-359.
13. Freeman, R. and I. Willner, *Optical molecular sensing with semiconductor quantum dots (QDs).* Chemical Society Reviews, 2012. **41**(10): p. 4067-4085.
14. Garnett, E., L. Mai, and P. Yang, *Introduction: 1D nanomaterials/nanowires.* Chemical reviews, 2019. **119**(15): p. 8955-8957.
15. Chen, C., et al., *One-dimensional nanomaterials for energy storage.* Journal of Physics D: Applied Physics, 2018. **51**(11): p. 113002.
16. Liu, J., et al., *Electrochemical fabrication of single-crystalline and polycrystalline Au nanowires: the influence of deposition parameters.* Nanotechnology, 2006. **17**(8): p. 1922.
17. Yu, X., et al., *Emergent pseudocapacitance of 2D nanomaterials.* Advanced Energy Materials, 2018. **8**(13): p. 1702930.
18. Zhu, C., et al., *3D printed functional nanomaterials for electrochemical energy storage.* Nano Today, 2017. **15**: p. 107-120.
19. Chinnasamy, C., et al., *Mixed spinel structure in nanocrystalline NiFe 2 O 4.* Physical Review B, 2001. **63**(18): p. 184108.
20. Thota, S. and S. Singh, *Nature of magnetic ordering in cobalt-based spinels.* Magnetic Spinels-Synthesis, Properties and Applications, 2017.
21. Sanchez-Lievanos, K.R., J.L. Stair, and K.E. Knowles, *Cation distribution in spinel ferrite nanocrystals: Characterization, impact on their physical properties, and opportunities for synthetic control.* Inorganic Chemistry, 2021. **60**(7): p. 4291-4305.
22. Gaudon, M., et al., *Structural defects in AFe2O4 (A= Zn, Mg) spinels.* Materials Research Bulletin, 2009. **44**(3): p. 479-484.
23. Mocala, K. and A. Navrotsky, *Structural and thermodynamic variation in nickel aluminate spinel.* Journal of the American Ceramic Society, 1989. **72**(5): p. 826-832.
24. Deraz, N., *Synthesis and characterization of nano-sized nickel aluminate spinel crystals.* International Journal of Electrochemical Science, 2013. **8**(4): p. 5203-5212.
25. Goswami, A., et al., *Novel applications of solid and liquid formulations of nanoparticles against insect pests and pathogens.* Thin solid films, 2010. **519**(3): p. 1252-1257.
26. Hachem, K., et al., *Methods of chemical synthesis in the synthesis of nanomaterial and nanoparticles by the chemical deposition method: A review.* BioNanoScience, 2022. **12**(3): p. 1032-1057.
27. Wang, Q., et al., *General synthesis of porous mixed metal oxide hollow spheres with enhanced supercapacitive properties.* ACS applied materials & interfaces, 2016. **8**(27): p. 17226-17232.
28. Fukuoka, A., et al., *Template synthesis of nanoparticle arrays of gold and platinum in mesoporous silica films.* Nano Letters, 2002. **2**(7): p. 793-795.
29. Davis, P.A. and C. Burns, *Photobiology in protected horticulture.* Food and Energy Security, 2016. **5**(4): p. 223-238.

30. Akhtar, K., et al., *Scanning electron microscopy: Principle and applications in nanomaterials characterization.* Handbook of materials characterization, 2018: p. 113-145.
31. Zygmuntowicz, J., A. Miazga, and K. Konopka, *Morphology of nickel aluminate spinel (NiAl2O4) formed in the Al2O3–Ni composite system sintered in air.* Compos Theory Pract, 2014. **14**(2): p. 106-10.
32. Jagadeeshwaran, C. and R. Murugaraj, *Structural, Optical, Magnetic, and Electrical Properties of Ni 0.5 Co 0.5 Al 2 O 4 System.* Journal of Superconductivity and Novel Magnetism, 2020. **33**: p. 1765-1772.
33. Wong, W.C., *Charge-exchange processes of titanium-doped aluminate crystals (aluminum (2) oxygen (3), yttrium (3) aluminum (5) oxygen (12), yttrium aluminum oxygen (3), magnesium aluminum (2) oxygen (4), lanthanum magnesium aluminum (11) oxygen (19))*. 1995: Princeton University.
34. Xie, R.J. and H.T. Hintzen, *Optical properties of (oxy) nitride materials: a review.* Journal of the American Ceramic Society, 2013. **96**(3): p. 665-687.
35. Shih, Y.-J., et al., *Electrochemical nitrate reduction as affected by the crystal morphology and facet of copper nanoparticles supported on nickel foam electrodes (Cu/Ni).* Chemical Engineering Journal, 2020. **383**: p. 123157.
36. Basak, M., et al., *The use of X-ray diffraction peak profile analysis to determine the structural parameters of cobalt ferrite nanoparticles using Debye-Scherrer, Williamson-Hall, Halder-Wagner and Size-strain plot: Different precipitating agent approach.* Journal of Alloys and Compounds, 2022. **895**: p. 162694.
37. Gao, X., et al., *Adsorption of heavy metal ions by sodium alginate based adsorbent-a review and new perspectives.* International journal of biological macromolecules, 2020. **164**: p. 4423-4434.
38. Nieto, C.H.D., et al., *Effect of temperature, current density and mass transport during the electrolytic removal of magnesium ions from lithium rich brines.* Desalination, 2022. **529**: p. 115652.
39. Muzayanha, S.U., et al., *A fast metals recovery method for the synthesis of lithium nickel cobalt aluminum oxide material from cathode waste.* Metals, 2019. **9**(5): p. 615.
40. Lassoued, A., et al., *RETRACTED ARTICLE: Synthesis and magnetic characterization of Spinel ferrites MFe 2 O 4 (M= Ni, Co, Zn and Cu) via chemical co-precipitation method.* Journal of Materials Science: Materials in Electronics, 2017. **28**: p. 18857-18864.
41. Bezrodna, T., et al., *IR-analysis of H-bonded H2O on the pure TiO2 surface.* Journal of Molecular Structure, 2004. **700**(1-3): p. 175-181.
42. Zurita-Mendez, N.N., et al., *Synthesis and characterization of nickel aluminate nanoparticles.* Materials Research Express, 2018. **6**(1): p. 015036.
43. Beg, S., N.A. Al-Areqi, and S. Haneef, *Study of phase transition and ionic conductivity changes of Cd-substituted Bi4V2O11− δ.* Solid State Ionics, 2008. **179**(39): p. 2260-2264.